J. M. Thomas, *Angew. Chem.* **1994**, *106*, 667–668; *Angew. Chem. Int. Ed. Engl.* **1994**, *33*, 639–641.
[5] M. A. Drezdzon, *Inorg. Chem.* **1988**, *27*, 4628–4632.
[6] A. K. Cheetham, G. Férey, T. Loiseau, *Angew. Chem.* **1999**, *111*, 3466–3492; *Angew. Chem. Int. Ed.* **1999**, *38*, 3268–3292.
[7] N. Guillou, Q. Gao, M. Nogues, R. E. Morris, M. Hervieu, G. Férey, A. K. Cheetham, *C. R. Acad. Sci. Paris* **1999**, *2*, 387–392.
[8] J.-S. Chang, S.-E. Park, Q. Gao, G. Férey, A. K. Cheetham, *Chem. Commun.* **2001**, *9*, 859–860.
[9] Thermodiffractometry was performed under air in an Anton Paar HTK16 high-temperature device of a Siemens D5000 X-ray powder diffractometer ($\theta-\theta$ mode; $Co_{K\alpha}$ radiation $\lambda = 1.7903$ Å), equipped with a M Braun linear position sensitive detector (PSD). Patterns were scanned with a resolution of 0.0147° and a divergence slit of 0.1° over an angular range of 5–50° (2θ), at 25 °C intervals up to 1000 °C; rate of increase of temperature: 0.1 °C s^{-1}; see Figure 1.
[10] TGA data were obtained on a TGA 2050 thermogravimetric analyser thermobalance using a sample synthesized by using 1,3-diaminopropane.
[11] BET analysis was performed by using a Micromeritics ASAP2400 porosimeter on a sample activated at 350 °C for four days.
[12] The X-ray powder diffraction data for VSB-5 were collected on a Siemens D5000 diffractometer by using $Cu_{K\alpha}$ radiation ($\lambda = 1.5418$ Å). To avoid preferred orientation effects, the synthesis was carried out under stirring conditions, keeping the same experimental conditions with the same molar ratio and filling rate. The resulting powder was then loaded in the sample holder. The powder diffraction pattern was scanned over an angular range of 4–120° (2θ). The counting times were 27 s per step to 59.98° (2θ) and 54 s per step from 60.00° (2θ) to the end of the scan (to improve the counting statistics of the high-angle region). The full pattern was then scaled to the lower counting time. An accurate determination of the peak positions and relative intensities was carried out by using the software package DIFFRACT-AT.
[13] A. Boultif, D. Louër, *J. Appl. Crystallogr.* **1991**, *24*, 987–993.
[14] A. Altomare, M. C. Burla, G. Cascarano, C. Giacovazzo, A. Guagliardi, A. G. G. Moliterni, G. Polidori, *J. Appl. Crystallogr.* **1995**, *28*, 842–846.
[15] A. Altomare, M. C. Burla, M. Camalli, G. L. Cascarano, C. Giacovazzo, A. Guargliardi, A. G. G. Moliterni, G. Polidori, R. Spagna. *J. Appl. Crystallogr.* **1999**, *32*, 115–119.
[16] J. Rodriguez-Carvajal, *Collected Abstracts of Powder Diffraction Meeting* (Toulouse, France) **1990**, p. 127.
[17] Further details on the crystal structure investigation may be obtained from the Fachinformationszentrum Karlsruhe, 76344 Eggenstein-Leopoldshafen, Germany (fax: (+49) 7247-808-666; e-mail: crysdata@fiz-karlsruhe.de), on quoting the depository number CSD-411917.
[18] Magnetization measurements were performed in the temperature range 4–295 K at 5 kG and 100 G on a Quantum Design Squid magnetometer (MPMS-5).
[19] The selective hydrogenation of 1,3-butadiene to butenes was carried out in a continuous fixed-bed reactor made of quartz at atmospheric pressure. Before catalytic measurement, the catalyst was reduced with 5% hydrogen in helium at 350 °C for 4–24 h. The reaction was carried out while introducing mixture of 1,3-butadiene (99.0%) and pure hydrogen under helium. The effluent stream from the reactor was analyzed by an on-line gas chromatograph (HP 5890 Series II) fitted with a capillary column (J&W Alumina) and a flame-ionization detector.
[20] H. Arnold, F. Doebert, J. Gaube in *Handbook of Heterogeneous Catalysis*, *Vol. 5* (Eds.: G. Ertl, H. Knoezinger, J. Weitkamp), VCH, Weinheim, **1997**, pp. 2165–2186.
[21] E. Iglesia, D. G. Barton, J. A. Biscardi, M. J. L. Gines, S. L. Soled, *Catal. Today* **1997**, *38*, 339–360.
[22] Decomposition of MBOH (>99%, Aldrich) was carried out in a plug-flow glass reactor with an internal diameter of 10 mm. The MBOH was placed in a vaporizer in which a helium flow was saturated with the alcohol vapor at 298 K and then the MBOH/helium mixture was fed into the reactor. The catalytic activity of VSB-5 was examined after the calcination of the fresh sample at 623 K for 4 h in air. Reaction products were analyzed by an on-line gas chromatograph (Hewlett-Packard model 5890II) fitted with a capillary column (J&W DB-WAX) and a flame-ionization detector.

Spherical Aromaticity of Inorganic Cage Molecules**

Andreas Hirsch,* Zhongfang Chen, and Haijun Jiao

We have shown recently that the icosahedral fullerenes C_{20}, C_{60}, and C_{80} reach maximum spherical aromaticity if their π shells are completely filled.[1] This is nicely demonstrated, for example, by the very pronounced diatropic character of the $2(N+1)^2$ π systems of the C_{20}^{2+} ($N=2$), C_{60}^{10+} ($N=4$), and C_{80}^{8+} ($N=5$) ions with perfect I_h symmetry. Here we extend this treatment of spherical aromaticity to a set of well-known inorganic cage compounds and demonstrate that they are highly aromatic because of the closed-shell nature of both their σ and π systems.

Tetrahedral clusters P_4 and As_4 form metastable solid allotropes, whereas Sb_4 and Bi_4 are high-temperature modifications existing only in liquid or in the gas phase. Tetrahedral N_4 (T_d), being the most stable singlet N_4 isomer,[2] was recently generated in a plasma as the first neutral polynitrogen species.[3] The calculated nucleus-independent chemical shifts (NICS)[4, 5] at the cage centers of these T_d-symmetrical clusters with optimized bond lengths (Figure 1)

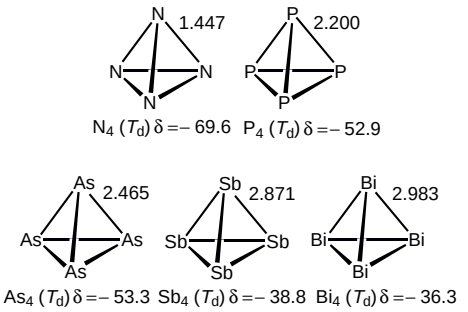

Figure 1. Optimized bond lengths [Å] and NICS values [δ] for E_4 (T_d) clusters (E = N, P, As, Sb, Bi).

are given in Table 1. The highly negative NICS values of all clusters are a result of pronounced diamagnetic ring currents. The pronounced diatropic character of these clusters is not a result of the addition of four individual increments consisting of three-membered rings, but a new quality of the entire cages. This is clearly reflected by the fact that: 1) the NICS and the NICS per valence electron (NICS/e) values in the center of the cages are considerably more negative than those in the

[*] Prof. Dr. A. Hirsch, Dr. Z. Chen, Dr. H. Jiao[+]
Institut für Organische Chemie der Universität Erlangen-Nürnberg
Henkestrasse 42
91054 Erlangen (Germany)
Fax: (+49) 9131-85-26864
E-mail: hirsch@organik.uni-erlangen.de
[+] Laboratoire de Chimie du Solide et Inorganique Moléculaire
UMR 6511 CNRS, Université de Rennes 1, Institut de Chimie de Rennes, 35042 Rennes Cedex (France)
[**] This work was supported by the Alexander von Humboldt Stiftung (Z. Chen), the Centre National de la Recherche Scientifique (H. Jiao), and the Fonds der Chemischen Industrie. We thank Prof. Dr. T. F. Fässler for his helpful discussion and reprints.

  1433-7851/01/4015-2834 $ 17.50+.50/0

Table 1. Calculated NICS values [δ] for E_4 (T_d), E_3H_3 (C_{3v}), and HE_4^+ (C_{3v}).

Type	NICS	Compound				
E_4[a]		N_4	P_4	As_4	Sb_4	Bi_4
	NICS[b]	−69.6	−52.9	−53.3	−38.8	−36.3
	NICS/e[c]	−3.5	−2.6	−2.7	−1.9	−1.8
	NICS[d]	−69.4	−52.3	−52.4	−38.7	−36.2
E_3H_3[a]		N_3H_3	P_3H_3	As_3H_3	Sb_3H_3	Bi_3H_3
	NICS[d]	−51.5	−33.5	−33.8	−26.6	−25.0
	NICS/e[c,d]	−2.9	−1.9	−1.9	−1.5	−1.4
HE_4^+[a]		HN_4^+	HP_4^+	HAs_4^+	HSb_4^+	HBi_4^+
	NICS[b]	−64.0	−40.4	−35.8	−22.1	−10.0

[a] All are energy minima. [b] At the cage center. [c] NICS per valence electron (NICS/e). [d] At the center (E_3) of the trigons.

center of the three-membered E_3H_3-rings (C_{3v}) (Table 1); 2) the NICS values in the center of the three-membered E_3H_3-rings (C_{3v}) are less negative than those in the center of the trigonal faces of E_4 (Table 1), and 3) the NICS/e values of four E_3H_3 increments at a location corresponding to the cage center of E_4 are considerably lower than those of the E_4 cage centers. For example the sum of the NICS/e values of four P_3H_3 units 0.45 Å away from the center of each plane which corresponds to the middle of the P_4 cage is $\delta = -1.3$ whereas that of P_4 itself is $\delta = -2.6$.

The calculated MO schemes of E_4 are in line with earlier calculations[6] and clearly reflect the closed-shell nature of both the σ and π subsystems (Figure 2). The σ system contains

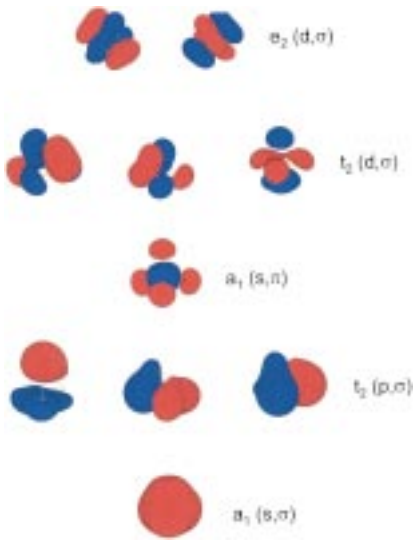

Figure 2. Representation of the MOs of P_4 (HyperChem 5.1). The a_1 (s,π) orbital is a cluster π orbital.[1, 7] As a result of the pyramidalization of the cluster atoms the endohedral overlap of atomic p orbitals is much more pronounced than the exohedral overlap.

$2(N_\sigma+1)^2$ σ electrons ($N_\sigma = 2$) and consists of a cluster s orbital, three degenerate cluster p orbitals, and two sets of cluster d orbitals (e and t_2), while the π system contains $2(N_\pi+1)^2$ π electrons ($N_\pi = 0$).[7] With respect to the model of the spherical electron gas,[1, 8] the splitting of the cluster d orbitals of σ systems is a consequence of symmetry lowering from K_h to T_d. With the complete filling of all σ and π shells the angular momenta are symmetrically distributed[1, 8] and the clusters are double spherically aromatic.[9] The HOMOs are the e (d,σ) orbitals (Figure 2). Electrons within the frontier region are the most mobile and contribute predominantly to the ring-current effect. Therefore, the diatropic character of these clusters is mainly determined by the σ electrons. Incomplete filling of the shells, accompanied by asymmetrical distribution of the angular momenta, causes reduction of aromatic character or even establishment of antiaromaticity. This is shown, for example, with the system P_4^{2-} where one of the three originally degenerate LUMOs of P_4 is occupied causing a symmetry lowering to C_{2v} (P–P = 2.159, 2.280, and 3.222 Å) and a NICS value of only $\delta = -23.0$; while the system P_4^{2+} has also lower symmetry (D_2, P–P = 2.168 and 2.670 Å) and a NICS value of $\delta = -15.6$.

The cluster ions Si_4^{4-}, Ge_4^{4-}, Sn_4^{4-}, and Pb_4^{4-}[10, 11] are isoelectronic with P_4, As_4, Sb_4, and Bi_4, have the same MO structure, and exhibit a comparable pronounced diatropic character and double spherical $2(N+1)^2$ aromaticity (Figure 3).

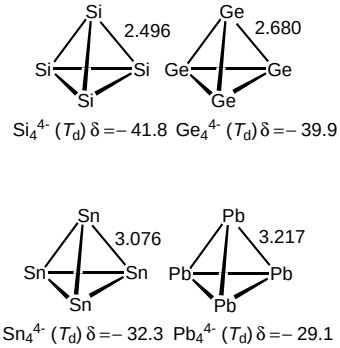

Figure 3. Optimized bond lengths [Å] and NICS values [δ] for E_4^{4-} (T_d) clusters (E = Si, Ge, Sn, Pb).

A set of less symmetrical clusters containing nine atoms is represented by the Zintl[12] ions shown in Figures 4–6 and Table 2. The D_{3h} symmetrical *closo*-cages E_9^{4-} (E = Si,[13] Ge,[14] Sn,[14c, 15] Pb[15e, 16]) and Bi_9^{5+}[17] (Figure 4) represent energy minima and do not obey the Wade rules.[18] A reason for their stability could be the double spherically $2(N+1)^2$ aromatic configuration of their valence-electron system containing 32 σ ($N_\sigma = 3$) and 8 π electrons ($N_\pi = 1$). In contrast to the T_d clusters (Figure 1 and 3) their MO schemes are characterized by a variety of crossovers between the subshells and a considerable decrease in orbital degeneracy of the completely filled σ (s, p, d, f) and π (s, p) levels. However, they still exhibit very high NICS values approaching those of some highly aromatic fullerenes with closed π shells.[1] The HOMO of these clusters is the a_2''(f,σ) orbital which corroborates earlier calculations.[19]

The corresponding *nido* structures with C_{4v} symmetry are slightly less stable (Figure 5, Table 2).[19] They are also double spherically $2(N+1)^2$ aromatic. Their HOMOs (f,σ), however, are two-fold degenerate.[19] E_9^{4-} clusters are known to be fluxional on the NMR time scale.[20] The D_{3h} cages can smoothly rearrange into the corresponding C_{4v} cages. Most of the corresponding Wade rule obeying *closo* cages E_9^{2-} (E = Sn, Pb)[21] and Bi_9^{7+} are unknown (Figure 6, Table 2), while

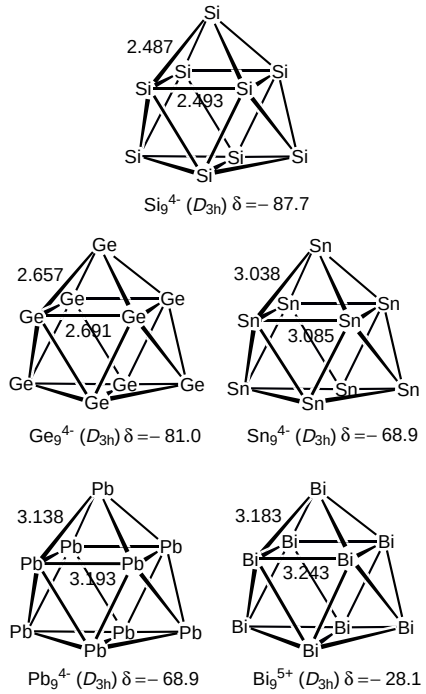

Figure 4. Optimized bond lengths [Å] and NICS values [δ] for E_9^{4-} (D_{3h}) clusters (E = Si, Ge, Sn, Pb) and Bi_9^{5+} (D_{3h}).

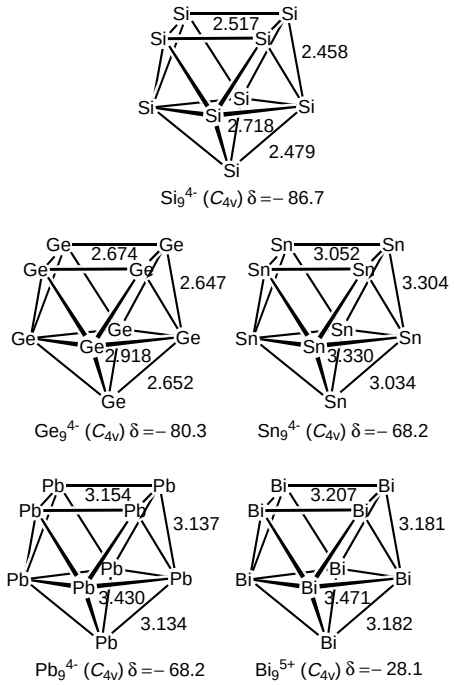

Figure 5. Optimized bond lengths [Å] and NICS values [δ] for E_9^{4-} (C_{4v}) clusters (E = Si, Ge, Sn, Pb) and Bi_9^{5+} (C_{4v}).

Ge_9^{2-} was reported.[14b] Noteworthy is that their σ shells are not completely filled, since the a_2''(f,σ) orbital is now empty leaving the a_2' (f,σ) as the HOMO.[19] As a consequence, the NICS values are considerably lower than those of the corresponding double $2(N+1)^2$ aromatic systems (Figure 4, Table 2). In all cases the HOMOs are σ orbitals and the π levels are inner-shell states.[19]

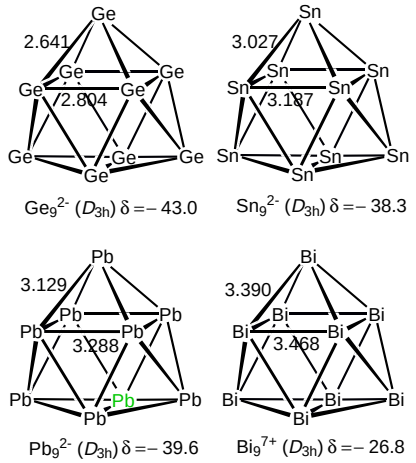

Figure 6. Optimized bond lengths [Å] and NICS values [δ] for E_9^{2-} clusters (D_{3h}) (E = Ge, Sn, Pb) and Bi_9^{7+} (D_{3h}).

Table 2. Calculated NICS values [δ] and relative energies E_{rel} [kcal mol^{-1}] for E_9^{4-}, E_9^{2-}, Bi_9^{5+}, and Bi_9^{7+}.

Species	symmetry	NICS	E_{rel}	Reference
Si_9^{4-}	*closo* (D_{3h})	– 87.7	0.0	[13]
	nido (C_{4v})	– 86.7	1.1	[13]
Ge_9^{4-}				
	closo (D_{3h})	– 81.0	0.0	[a]
	nido (C_{4v})	– 80.3	0.8	[14]
Sn_9^{4-}	*closo* (D_{3h})	– 68.9	0.0	[a]
	nido (C_{4v})	– 68.2	0.8	[14c, 15]
Pb_9^{4-}	*closo* (D_{3h})	– 68.9	0.0	[16]
	nido (C_{4v})	– 68.3	1.0	[15e, 16]
Bi_9^{5+}	*closo* (D_{3h})	– 28.1	0.0	[17]
	nido (C_{4v})	– 28.1	0.4	[a]
Ge_9^{2-}	*closo* (D_{3h})	– 43.0	–	[14b]
Sn_9^{2-}	*closo* (D_{3h})	– 38.3	–	[a]
Pb_9^{2-}	*closo* (D_{3h})	– 39.6	–	[a]
Bi_9^{7+}	*closo* (D_{3h})	– 26.8	–	[a]

[a] Unknown experimentally.

Protonation of E_4 (E = N, P, As, Sb, Bi) leading to the isoelectronic C_{3v}-symmetrical cages HE_4^+ causes a reduction of the NICS values (i.e. becomes less negative) because of a reduction of electron mobility (Table 1). However, especially the clusters HE_4^+ (E = N, P, As) are still highly aromatic. The corresponding cluster σ and π orbitals[7] are closely related to those of the parent E_4 cages. The only difference is the presence of the exohedral protons, making the H–E fragments *pseudo* cluster atoms.[7] The complete protonation of all cluster atoms is realized in the *closo*-boranes $B_nH_n^{2-}$ (n = 5–12). As reported by Schleyer and Najafian,[22] the *closo*-boranes $B_nH_n^{2-}$ are highly diatropic with NICS values of the cluster centers ranging from $\delta = -24.5$ to -34.4. The closed-shell nature of O_h $B_6H_6^{2-}$, for example, is realized with $2(N_\pi+1)^2$ π electrons ($N_\pi = 1$) and $2(N_\sigma+1)^2$ σ electrons ($N_\sigma = 2$; Figure 7). The I_h-symmetrical $B_{12}H_{12}^{2-}$ ion contains $(N_\pi+1)^2$ π electrons ($N_\pi = 2$) and $2(N_\sigma+1)^2$ σ electrons ($N_\sigma = 3$). Note that these two highly symmetrical systems are double spherical aromatic and exhibit the highest NICS values in this series.[22]

In contrast to the carbon-based fullerene clusters the HOMOs within the highly symmetrical inorganic cage com-

  1433-7851/01/4015-2836 $ 17.50+.50/0 *Angew. Chem. Int. Ed.* **2001**, *40*, No. 15

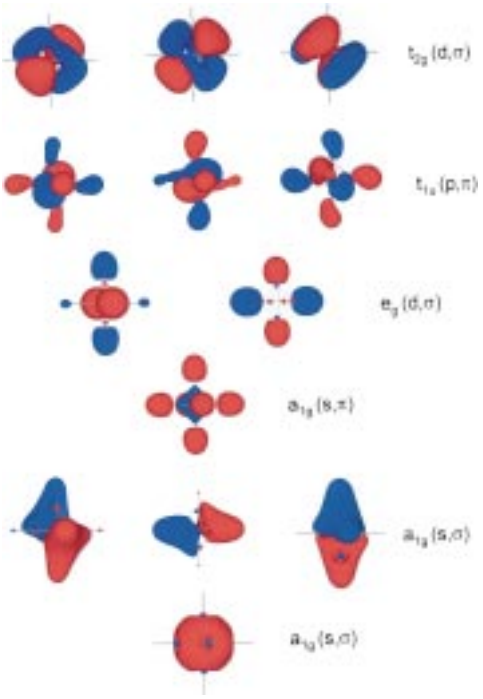

Figure 7. Representation of the MOs of $B_6H_6^{2-}$ (HyperChem 5.1).

pounds investigated here are σ orbitals. Like the spherical $2(N_\pi+1)^2$ aromaticity of the fullerenes the double spherical aromaticity of inorganic cage compounds involving both the whole π and σ system is a consequence of complete filling of the corresponding shells that can be deduced with group theory from molecular s, p, d, ⋯ shells of a spherical electron gas by reduction of the K_h symmetry to the cluster symmetry under consideration. As we will show in an forthcoming publication small and less symmetrical clusters such as Bi_5^{3+} do not obey the $2(N+1)^2$ rule and their aromaticity is reduced compared to systems with completely filled shells. However, we will also demonstrate that the spherical electron gas model[1, 8] that we used to deduce the $2(N+1)^2$ count rule forms the basis to treat any cluster type with a closed-cage structure. It can even be used by symmetry lowering to deduce the Hückel count rule for the cyclic annulenes. This leads to a unified picture of aromaticity and understanding of the special stability and reactivity of nonorganic molecules.[23]

Received: January 5, 2001
Revised: May 10, 2001 [Z16375]

[1] A. Hirsch, Z. Chen, H. Jiao, *Angew. Chem.* **2000**, *112*, 4079 – 4081; *Angew. Chem. Int. Ed.* **2000**, *39*, 3915 – 3917.

[2] a) M. N. Glukhovtsev, H. Jiao, P. von R. Schleyer, *Inorg. Chem.* **1996**, *35*, 7124 – 7133; b) K. Kobayashi, H. Miura, S. Nagase, *J. Mol. Struct. (THEOCHEM)* **1994**, *117*, 69 – 77.

[3] J. P. Zheng, J. Waluk, J. Spanget-Larsen, D. M. Blake, J. George Radziszewski, *Chem. Phys. Lett.* **2000**, *328*, 227 – 233.

[4] NICS-*N*ucleus *I*ndependent *C*hemical *S*hifts: P. von R. Schleyer, C. Maerker, A. Dransfeld, H. Jiao, N. J. R. van Eikema Hommes, *J. Am. Chem. Soc.* **1996**, *118*, 6317 – 6318.

[5] Geometry optimizations and frequency calculations were carried out at the B3LYP density functional level of theory with the 6 – 311 + G** basis set for E = N, P, As, Si, Ge; and LANL2DZp basis set for E = Sb, Bi, Sn, Pb; a) P. J. Hay, W. R. Wadt, *J. Chem. Phys.* **1985**, *82*, 299; b) T. H. Dunning, Jr., P. J. Hay, *Modern Theoretical Chemistry*, (Ed.: H. F. Schaefer III), Plenum, New York, **1976**, p. 1. For polarization functions see: S. Huzinaga, J. Anzelm, M. Klobukowski, E. Radzio-Andzelm, Y. Sakai, H. Tatewaki, *Gaussian Basis Sets for Molecular Calculations*, Elsevier, Amsterdam, **1984**. NICS were calculated at the same level with the same corresponding basis sets and optimized geometries. All calculations were done with the Gaussian 98 (Revision A.7), M. J. Frisch, G. W. Trucks, H. B. Schlegel, G. E. Scuseria, M. A. Robb, J. R. Cheeseman, V. G. Zakrzewski, J. A. Montgomery, R. E. Stratmann, J. C. Burant, S. Dapprich, J. M. Millam, A. D. Daniels, K. N. Kudin, M. C. Strain, O. Farkas, J. Tomasi, V. Barone, M. Cossi, R. Cammi, B. Mennucci, C. Pomelli, C. Adamo, S. Clifford, J. Ochterski, G. A. Petersson, P. Y. Ayala, Q. Cui, K. Morokuma, D. K. Malick, A. D. Rabuck, K. Raghavachari, J. B. Foresman, J. Cioslowski, J. V. Ortiz, B. B. Stefanov, G. Liu, A. Liashenko, P. Piskorz, I. Komaromi, R. Gomperts, R. L. Martin, D. J. Fox, T. Keith, M. A. Al-Laham, C. Y. Peng, A. Nanayakkara, C. Gonzalez, M. Challacombe, P. M. W. Gill, B. G. Johnson, W. Chen, M. W. Wong, J. L. Andres, M. Head-Gordon, E. S. Replogle, J. A. Pople, Gaussian, Inc., Pittsburgh, PA, **1998**..

[6] H. Zhang, K. Balasubramanian, *J. Chem. Phys.* **1992**, *97*, 3437 – 3444.

[7] In analogy to the nonplanar fullerenes (see ref. [1] and P. C. Haddon, *Science* **1993**, *261*, 1545 – 1550) a cluster π orbital is defined as an orbital containing a nodal plane spanned by all cluster heavy atoms. A similar definition which also allows the presence of protons within the mobile electron system (*closo*-boranes, CH^+ fragments) is given in T. A. Albright, J. K. Burdett, M.-H. Whangbo, *Orbital Interactions in Chemistry*, Wiley, New York, **1985**.

[8] A. Hirsch, *Top. Curr. Chem.* **1999**, *199*, 1 – 65. In addition to our inert-gas model and electron-counting rule for fullerene chemistry, there are highly related electron-counting rules for understanding the structures and bonding of transition metal clusters and various boron hydrides. For example, the tensor surface harmonic (TSH) theory which considers a molecule (or a cluster of atoms) as a central atom surround by a sphere of electron density, which is representative of the ligand co-ordination sphere. This leads to an approximate classification of the cluster orbitals in terms of angular momentum quantum numbers (we thank one referee for pointing out the spherical shell model which has the magic number of electrons (2, 8, 20, 40, 70, …, and the possibilities in-between e.g., 10, 18, 26, 34, …). For theoretical background and applications, see: A. J. Stone, *Mol. Phys.* **1980**, *41*, 1339 – 1354; A. J. Stone, *Inorg. Chem.* **1981**, *20*, 563 – 571; A. J. Stone, *Polyhedron* **1984**, *3*, 1299 – 1306; A. J. Stone, M. J. Alderton, *Inorg. Chem.* **1982**, *21*, 2297 – 2302). This theory has been generalized and extended (*Complementary Spherical Electron Density Model*) by D. M. Mingos, J. C. Hawes in *Structure and Bonding*, Springer, Berlin, **1985**, p. 1 – 63, and references therein. For further applications, see: P. W. Fowler, *Polyhedron* **1985**, *4*, 2051 – 2057; D. B. Redmond, *J. Chem. Soc. Faraday Trans.* **1983**, *79*, 1791 – 1809.

[9] Double aromaticity for planar systems, see: P. von R. Schleyer, H. Jiao, M. N. Glukhovtsev, J. Chandrasekhar, E. Kraka, **1994**, *116*, 10129 – 10134.

[10] I. F. Hewaidy, E. Busmann, W. Klemm, *Z. Anorg. Allg. Chem.* **1964**, *328*, 283 – 293.

[11] a) H. Schäfer, *Annu. Rev. Mater. Sci.* **1985**, *15*, 1 – 41; b) G. Kliche, M. Schwarz, H. G. von Schnering, *Angew. Chem.* **1987**, *99*, 350 – 352; *Angew. Chem. Int. Ed. Engl.* **1987**, *26*, 349 – 351.

[12] For some recent reviews, see: a) J. D. Corbett, *Angew. Chem.* **2000**, *112*, 682 – 704; *Angew. Chem. Int. Ed.* **2000**, *39*, 670 – 690; b) J. D. Corbett, *Struct. Bonding (Berlin)* **1997**, *87*, 157 – 193; c) J. D. Corbett, *Chemistry, Structures and Bonding of Zintl Phases and Ions* (Ed.: S. Kauzlarich), VCH, New York, **1996**, chap. 3. d) J. D. Corbett, *Chem. Rev.* **1985**, *85*, 383 – 397.

[13] a) H. G. von Schnering, M. Somer, M. Kaupp, W. Carrillo-Cabrera, M. Baitinger, A. Schmeding, Y. Grin, *Angew. Chem.* **1998**, *100*, 1507 – 2509; *Angew. Chem. Int. Ed.* **1998**, *37*, 2359 – 2361; b) V. Queneau, E. Todorov, S. C. Sevov, *J. Am. Chem. Soc.* **1998**, *120*, 3263 – 3264.

[14] a) V. Queneau, S. C. Sevov, *Angew. Chem.* **1997**, *109*, 1818 – 1820; *Angew. Chem. Int. Ed. Engl.* **1997**, *36*, 1754 – 1756; b) C. H. E. Belin, J. D. Corbett, A. Cisar, *J. Am. Chem. Soc.* **1977**, *99*, 7163 – 7169; c) H. G. von Schnering, M. Baitinger, U. Bolle, W. Carrillo-Cabrera, J. Curda, Y. Grin, F. Heinemann, J. Llanos, K. Peters, A. Schmeding, M.

  1433-7851/01/4015-2837 $ 17.50+.50/0

Somer, *Z. Anorg. Allg. Chem.* **1997**, *623*, 1037 – 1039. For some discussions on the paramagnetic E_9^{3-} and $[E_9E_9]^{6-}$ ions (E = Ge, Sn, Pb), see: d) T. F. Fässler, M. Hunziker, *Inorg. Chem.* **1994**, *33*, 5380 – 5381; e) T. F. Fässler, U. Schütz, *Inorg. Chem.* **1999**, *38*, 1866 – 1870; f) T. F. Fässler, M. Hunziker, *Z. Anorg. Allg. Chem.* **1996**, *622*, 837 – 844; g) T. F. Fässler, H.-J. Muhr, M. Hunziker, *Eur. J. Inorg. Chem.* **1998**, 1433 – 1438; h) T. F. Fässler, M. Hunziker, M. E. Spahr, *Z. Anorg. Allg. Chem.* **2000**, *626*, 692 – 700, and references therein.

[15] a) J. D. Corbett, P. A. Edwards, *J. Am. Chem. Soc.* **1977**, *99*, 3313 – 3317; b) D. Kummer, L. Diehl, *Angew. Chem.* **1970**, *82*, 881 – 882; *Angew. Chem. Int. Ed. Engl.* **1970**, *9*, 895; c) B. W. Eichhorn, R. Haushalter, W. T. Pennington, *J. Am. Chem. Soc.* **1988**, *110*, 8704 – 8706; d) R. Burns, J. D. Corbett, *Inorg. Chem.* **1985**, *24*, 1489 – 1492; e) N. Korber, A. Fleischmann, *J. Chem. Soc. Dalton Trans.* **2001**, 383 – 385.

[16] a) V. Queneau, S. C. Sevov, *Inorg. Chem.* **1998**, *37*, 1358 – 1360; b) E. Todorov, S. C. Sevov, *Inorg. Chem.* **1998**, *37*, 3889 – 3891; c) J. Campbell, D. A. Dixon, H. P. A. Mercier, G. J. Schrobilgen, *Inorg. Chem.* **1995**, *34*, 5798 – 5809.

[17] R. M. Friedman, J. D. Corbett, *Inorg. Chem.* **1973**, *12*, 1134 – 1139.

[18] M. E. O'Neill, K. Wade, *J. Mol. Struct.* **1983**, *103*, 259 – 268.

[19] L. L. Lohr, Jr., *Inorg. Chem.* **1981**, *20*, 4229 – 4235.

[20] a) R. W. Rudolph, W. L. Wilson, F. Parker, R. C. Taylor, D. C. Young, *J. Am. Chem. Soc.* **1978**, *100*, 4629 – 4630; b) R. W. Rudolph, W. L. Wilson, R. C. Taylon, *J. Am. Chem. Soc.* **1981**, *103*, 2480 – 2481.

[21] One referee asked about the sources of the disagreement between theory and experiment: the major problems are 1) the quality of the crystals, the role of the counter ions, and packing in the solid states; 2) the choice of model system, the effect of electron correlation, and the size of the employed basis set including relativistic correction.

[22] P. von R. Schleyer, K. Najafian, *Inorg. Chem.* **1998**, *37*, 3454 – 3470.

[23] X. Li, A. E. Kuznetsiv, H.-F. Zhang, A. I. Bodyrev, L.-S. Wang, *Science* **2001**, *291*, 859 – 861; b) D.-K. Seo, J. D. Corbett, *Science* **2001**, *291*, 841 – 842.

  1433-7851/01/4015-2838 $ 17.50+.50/0